Naval Research Laboratory

Washington, DC 20375-5320

NRL/MR/6794--97-7893

Electrostatic Particle-in-Cell Simulation Technique for Quasineutral Plasma

GLENN JOYCE
MARTIN LAMPE
STEVEN P. SLINKER
WALLACE M. MANHEIMER

Beam Physics Branch
Plasma Physics Division

March 31, 1997

REPORT DOCUMENTATION PAGE

Form Approved
OMB No. 0704-0188

1. AGENCY USE ONLY (*Leave Blank*)	2. REPORT DATE	3. REPORT TYPE AND DATES COVERED
	March 31, 1997	Interim Report

4. TITLE AND SUBTITLE

Electrostatic Particle-in-Cell Simulation Technique for Quasineutral Plasma

5. FUNDING NUMBERS

6. AUTHOR(S)

Glenn Joyce, Martin Lampe, Steven P. Slinker, and Wallace M. Manheimer

7. PERFORMING ORGANIZATION NAME(S) AND ADDRESS(ES)

Naval Research Laboratory
Washington, DC 20375-5320

8. PERFORMING ORGANIZATION REPORT NUMBER

NRL/MR/6794--97-7893

9. SPONSORING/MONITORING AGENCY NAME(S) AND ADDRESS(ES)

Office of Naval Research
Arlington, VA 22217

10. SPONSORING/MONITORING AGENCY REPORT NUMBER

11. SUPPLEMENTARY NOTES

12a. DISTRIBUTION/AVAILABILITY STATEMENT

Approved for public release; distribution unlimited.

12b. DISTRIBUTION CODE

13. ABSTRACT (*Maximum 200 words*)

We have developed a particle-in-cell simulation method in which the electrostatic field is determined from the requirement of quasineutrality, rather than Poisson's equation. Time steps may be orders of magnitude longer than the plasma period, and mesh cells orders of magnitude longer than the Debye length, since electron plasma oscillations do not appear in the model and the Debye length is essentially set to zero. The quasineutral approach also avoids the problem of statistical fluctuations in the charge density, which frustrate the use of Poisson's equation in a quasineutral plasma. The simulation technique correctly represents kinetic features such as Landau damping. The method is demonstrated by application to several simple test problems, including free expansion of a plasma, and linear and nonlinear ion sound. In the case of a plasma with strongly magnetized electrons, we apply the technique to determine the parallel electric field and parallel transport within the plasma. Quasineutral techniques for representing cross-field transport, and edge effects in bounded plasmas, will be discussed in subsequent publications.

14. SUBJECT TERMS

Quasineutral plasma
Plasma simulation
Particle simulation
Particle-in-cell simulation

15. NUMBER OF PAGES

38

16. PRICE CODE

17. SECURITY CLASSIFICATION OF REPORT	18. SECURITY CLASSIFICATION OF THIS PAGE	19. SECURITY CLASSIFICATION OF ABSTRACT	20. LIMITATION OF ABSTRACT
UNCLASSIFIED	UNCLASSIFIED	UNCLASSIFIED	UL

NSN 7540-01-280-5500

Standard Form 298 (Rev. 2-89)
Prescribed by ANSI Std 239-18
298-102

CONTENTS

ELECTROSTATIC PARTICLE-IN-CELL SIMULATION TECHNIQUE FOR QUASINEUTRAL PLASMA

1. Introduction

In particle-in-cell (PIC) simulations of plasmas, the standard technique[1-3] for calculating the electrostatic field is to solve Poisson's equation, with the charge density source term determined by the laydown of the densities of electrons and ions, n_e and n_i. This procedure works well when the phenomena of interest proceed on time scales comparable to the electron plasma frequency ω_p and spatial scales comparable to the Debye length λ_D, and when there is substantial charge separation between electrons and ions. However, there are many plasma problems where the time and space scales are very much longer, and where the plasma maintains quasineutrality throughout, i.e. $|n_e-n_i| << n_i$. In these situations, it can be extraordinarily inefficient, or even unfeasible, to use Poisson's equation.

One problem is that the simulation supports electron plasma oscillations, and therefore the time step must be less than $2\omega_p^{-1}$ for stability.[4] In many situations, electron oscillations play no role in the phenomena of interest, and the shortest time scale that is actually of interest may be the period of a low-frequency wave, an ion time scale, a collisional time scale, or a time scale for electron transport over some macroscopic length. These time scales may be several orders of magnitude longer. Implicit algorithms[5-11] have often been used to avoid resolution of the electron plasma oscillation time scale. However, PIC simulation techniques also face a more fundamental difficulty arising from the circumstances of quasineutrality. The charge separation between electrons and ions, $n_e - n_i$, is often less than 10^{-5} of the density of either electrons or ions. If the electrons and ions are represented by simulation macroparticles, any attempt to calculate the potential directly from Poisson's equation would be futile, and overwhelmed by statistical noise. For example, in a million-particle 2D simulation with a 100 X 100 grid, there are typically 100 macroparticle electrons or ions in each cell. The physically correct value of the difference between the number of electrons and ions in the cell would be on the order of 10^{-3} macroparticles, clearly unresolvable, whereas the statistical fluctuations within the cell would be on the order of $\sqrt{100}$ macroparticles, which is four orders of magnitude larger than the actual value. Numerical schemes involving Poisson's

Manuscript approved November 1, 1996

equation are obviously very difficult (and actually inappropriate) in the quasineutral limit. Indeed, Chen[12] noted long ago that, "In a plasma, it is usually possible to assume $n_e = n_i$ and $\nabla \cdot \mathbf{E} \neq 0$ at the same time. This is a fundamental trait of plasmas, one which is difficult for the novice to understand. *Do not use Poisson's equation to obtain E unless it is unavoidable!"*

Over the years, this advice has been applied in many analytic and numerical models which represent the plasma as a fluid, or represent the electrons as either a dielectric medium or a fluid within some hybrid scheme.[13-15] Methods have been developed which circumvent the use of Poisson's equation by neglecting electron inertia and determining **E** from the resulting simplified electron momentum conservation equation. In these models, n_i is determined from dynamical equations, but n_e is not separately calculated; it is simply set equal to n_i to maintain quasineutrality. This procedure eliminates temporal scales on the order of the electron plasma frequency, as well as spatial structures on the Debye length scale. However, in fully kinetic models, and in particular in PIC simulations, the electron density is calculated directly by the simulation, and the usual approach has been to calculate ϕ from Poisson's equation.

We have developed a new approach to the simulation of quasineutral plasmas with particle electrons and particle ions. Our approach is motivated by the quasineutral fluid techniques described in the previous paragraph, and our objective is to use grid spacing wide compared to the Debye length, and time steps long compared to the electron plasma frequency. We believe that the technique can be used to treat a wide variety of plasma problems. However, the primary objective of our present work is multi-dimensional overall modeling of an electron cyclotron resonance (ECR) reactor used for plasma processing. The plasma in this case is bounded, partially ionized, collisional, and magnetized, with a typical plasma density 10^{12} cm^{-3}, electron temperature several eV, and neutral density several times 10^{13}. The scale size of the reactor is tens of cm ($>10^3\lambda_D$), and the time scales of interest range from 10 ns (electron transit times over cm size features, and electron collision times) to hundreds of μs (chemical equilibration), while $\lambda_D \cong 10^{-3}$ cm $\omega_p^{-1} \cong 10^{-11}$ sec. In recent years, there has been considerable interest in the use of particle-in-cell/Monte Carlo (PIC/MC) codes to model this type of plasma.[16-25].

Like pure PIC codes, these have typically used Poisson's equation to determine the electric field. In the present paper, we discuss only the method for determining the internal electric field within an unmagnetized bulk plasma, or parallel to the magnetic field in a magnetized bulk plasma. In subsequent publications, we shall discuss self-consistent techniques for dealing with sheaths, collisions and chemistry, and with cross-field transport in a magnetized plasma, within a multidimensional quasineutral framework.

2. Calculation of the Electric Field

A. Unmagnetized One-Dimensional Plasma

For simplicity, we shall consider a one-dimensional system specified by Cartesian coordinate z, although the formalism can be extended to multi-dimensional systems. We assume that the simulation is globally quasineutral, i. e. the total number of electrons is equal to the total number of ions. We also assume that the electron Debye length is small compared to any scale length resolved in the model, and the electron plasma frequency is fast compared to any time scale resolved in the model. Thus, if there were any departure from local quasineutrality, the resulting strong electric field would drive electron currents to restore quasineutrality within a time scale of several electron plasma periods, i.e., essentially instantaneously on the time scale of the model. Thus, the electric field always takes the value necessary to keep the electron density n_e equal to the ion density n_i. To specify this electric field, we can begin with the electron momentum conservation equation,

$$-eE = \frac{1}{n_e}\frac{\partial P_e}{\partial z} + \nu_e m_e u_e + \frac{1}{n_e}\frac{\partial}{\partial t}\left(n_e m_e u_e\right). \tag{1}$$

Here, $P_e(z,t)$, $u_e(z,t)$ and $\nu_e(z,t)$ are the electron kinetic pressure (including flow terms), the electron fluid velocity, and the mean electron momentum transfer collision frequency, which can be specified as integrals over the electron distribution function $f_e(z,v,t)$,

$$P_e(z,t) \equiv \int dv\, m_e v^2 f_e(z,v,t), \tag{2a}$$

$$u_e(z,t) \equiv \int dv\, v f_e(z,v,t), \tag{2b}$$

$$\nu_e(z,t) \equiv \int dv\, \nu(z,v,t) f_e(z,v,t). \tag{2c}$$

These integrals, which appear in the first two terms on the right hand side of Eq. (1), can be evaluated at each point of the grid, by laying down the mean quantities for the electrons assigned to that grid point. [The collision frequency $\nu(z,v,t)$ represents a sum over the various collisional processes which are represented in the simulation as Monte Carlo events, dynamical friction, etc.]

The first two terms on the right-hand side of (1) represent the ambipolar electric field, which balances the electron pressure gradients, flow gradients, and frictional forces. For low-frequency plasma processes which maintain quasineutrality (the only type of processes we wish to follow), the inertial term [last term of Eq. (1)] is smaller by order m_e/m_i. In a quasineutral *fluid* formulation, the inertial term would be neglected, and the ambipolar field would be used in the ion dynamical equations to calculate n_i at the next time step. Then n_e would simply be set equal to n_i. However, this is not quite sufficient in a particle simulation, where the electrons and ions evolve separately during each time step. With E set equal to the ambipolar field, $n_e(z,t)$ remains constant in time (except for statistical fluctuations), while the ion density $n_i(z,t)$ gradually evolves because of the relatively slow ion motion. Thus the ambipolar field alone will not maintain the quasineutrality relation

$$n_e(z,t) = n_i(z,t). \tag{3}$$

Even worse, particle simulations are always subject to statistical fluctuations in the density and flux of any species at any given grid point, typically of the order of $\sqrt{N}$, where N is the number of particles in a grid site. Thus, a particle simulation code must

contain some mechanism for stably maintaining the quasineutrality relation (3) in the face of these fluctuations, which are of much larger order than m_e/m_i.

We have found that for low-frequency phenomena the kinetic information of interest is essentially contained in the ambipolar field, and that the last term of (1) serves only the functional purpose of keeping n_e equal to n_i. This opens up the possibility of keeping the ambipolar field but using an approximate technique to maintain Eq. (3), rather than calculating the actual inertial term. In earlier work,[26] we have experimented with the technique of pushing the both the electrons and ions in the ambipolar field alone, and then applying an approximate correction field to the electrons which restores the quasineutrality condition. This worked well, and we were able to prove that kinetic properties such as the Landau damping of ion sound waves were preserved. However, this approach can become somewhat complicated, especially when care is taken to conserve energy exactly. In the present paper, we describe an approach which is even simpler, works extremely well over very long times, and has excellent stability and energy conservation properties. This approach is simply to replace Eq. (1) with a modified form of the ambipolar field,

$$-eE = \frac{1}{n_i}\frac{\partial}{\partial z}\left(n_i T_e\right) + \nu_e m_e u_e, \tag{4}$$

where the electron kinetic pressure $P_e(z,t) \equiv n_e(z,t)T_e(z,t)$ is replaced by $n_i(z,t)T_e(z,t)$, using the *ion* density instead of n_e. Here, T_e is a kinetic temperature (including flow terms), defined as

$$n_e(z,t)T_e(z,t) \equiv \int dv m_e v^2 f_e(z,v,t). \tag{5}$$

This simple artifice causes the electron density to remain closely coupled to the ion density. This can be seen by writing the electron momentum conservation equation in the form

$$m_e \frac{\partial u_e}{\partial t} + \frac{1}{n_e}\frac{\partial}{\partial z}(n_e T_e) + eE + \nu_e m_e u_e = 0. \tag{6}$$

Using Eq. (4) for E, this gives

$$m_e \frac{\partial u_e}{\partial t} = T_e \frac{\partial}{\partial z} \ell n\left(\frac{n_i}{n_e}\right). \tag{7}$$

Equation (7) shows that the electrons are always accelerated up the gradient n_i/n_e i.e. toward the point of maximum positive charge density. The result is that the electron density oscillates about the ion density. Although these oscillations are unphysical, they are rapid and the oscillation amplitude should remain small if the system is started in a quasineutral state and the time step is small enough. The stability properties of these oscillations will be discussed in Sec. 3, and examples will be given in Secs. 5 and 6.

B. Strongly Magnetized Electrons

In the application which we are studying, ECR plasma sources, the electrons are strongly magnetized, with gyrofrequencies comparable to ω_p and gyroradii comparable to the Debye length. Since we do not wish to resolve these short time and space scales, it is convenient to use a guiding center representation of the electrons. An electron is characterized by its coordinate ζ, the curvilinear coordinate along the field line, its parallel velocity $v_\parallel \equiv d\zeta/dt$, and the magnitude $v_\perp$ of its perpendicular velocity. However, in practice is more convenient to use the electron's magnetic moment $\mu \equiv mv_\perp^2/2B$ as the independent variable, rather than $v_\perp$, since μ is an adiabatic invariant. Here, B is the magnitude of the magnetic field. The equation of motion for an electron, between collisions, includes a mirror force term and is

$$\frac{dv_\parallel}{dt} = -eE_\parallel - \mu\frac{\partial B}{\partial \zeta}. \tag{8}$$

Within our quasineutral formulation, the electric field component parallel to **B** is then specified by the electron momentum equation in the form

$$-eE_{\parallel} = \frac{B}{n_e}\frac{\partial}{\partial\zeta}\frac{P_{e\parallel}}{|B|} + \mu\frac{-\partial B}{\partial\zeta} + \nu_e m_e u_{e\parallel} + \frac{1}{n_e}\frac{\partial}{\partial t}\left(n_e m_e u_{e\parallel}\right), \tag{9}$$

where $P_{e\parallel}$ and $P_{e\perp}$ are the electron kinetic pressure parallel and perpendicular to **B**, and $\bar{\mu} \equiv T_{e\perp}/B$ is the mean magnetic moment for electrons at a given location. [Note that the mirror force vanishes from Eq. (9) if $P_{e\parallel} = P_{e\perp}$.] As in the previous section, we simply drop the inertial term in (9) and replace $P_{e\parallel}$ by $n_i T_e$, so that $E_\parallel$ is specified by the equation

$$-eE_{\parallel} = \frac{B}{n_i}\frac{\partial}{\partial\zeta}\frac{n_i T_{e\parallel}}{|B|} + \mu\frac{-\partial B}{\partial\zeta} + \nu_e m_e u_{e\parallel}. \tag{10}$$

The determination of the transverse electric field $E_\perp$ involves the ion dynamics and, in the case of a bounded plasma in a conducting vessel, also couples to the sheath potentials. This will be discussed in a subsequent publication.

3. Formal Analysis of Mode Structure and Stability

A. Linearized Normal Modes

To elucidate the way in which the electric field from Eq. (4) or Eq. (10) couples the electron and ion densities, we shall examine the linear normal modes supported by the system. Assuming an equilibrium with uniform density n_0 and temperature T_0, linearizing Eq. (4), assuming normal modes of the form $e^{i(kz-\omega t)}$, and neglecting collisions, we have

$$-eE = ikT_e + \frac{ikT_0}{n_0}n_i. \tag{11}$$

In this analysis, we use linearized cold fluid equations for the ions, so that

$$n_i = \frac{ikn_0 eE}{\omega^2 m_i}. \tag{12}$$

Combining Eqs. (11) and (12), we find

$$eE = -\frac{ikT_e}{1 - k^2 c_s{}^2/\omega^2}. \tag{13}$$

To complete the analysis, we use the linearized Vlasov equation for the electrons,

$$\frac{\partial f_e}{\partial t} + v\frac{\partial f_e}{\partial z} - \frac{n_0 eE}{m_e}\frac{\partial F_0}{\partial v} = 0, \tag{14}$$

where $F_0(v)$ is the normalized equilibrium electron velocity distribution and $f_e(z,v,t)$ is now the first-order perturbation. Using (13) in (14), we find

$$f_e = -\frac{T_e}{m_e}\,\frac{1}{1 - k^2 c_s{}^2/\omega^2}\,\frac{F_0'(v)}{v - \omega/k}. \tag{15}$$

T_e can be calculated by using

$$n_e = \int dv\, f_e(v) \tag{16}$$

and

$$n_e T_0 + n_0 T_e = \int dv\, mv^2 f_e(v). \tag{17}$$

Using (16) and (17) in (15) yields a dispersion relation

$$1-\frac{k^2 c_s^{\,2}}{\omega^2}+\int \frac{dv(v^2-v_e^{\,2})F_0'(v)}{v-\omega/k}=0. \tag{18}$$

We note first that if $c_s \to 0$, so that the ions are immobile, then

$$\omega = \pm k v_e \tag{19}$$

is a pair of exact solutions of Eq. (18). Here, $v_e \equiv \sqrt{T_e / m_e}$ is the electron thermal velocity. This mode represents the unphysical high frequency oscillations that keep the electron density closely coupled to the ion density. However, the oscillation frequency ω is much smaller than ω_p. In a simulation with spatial grid scale Δz, the frequency is limited to $\omega < v_e/\Delta z$, and if there is any spatial smoothing the highest-k modes are strongly damped, so that the highest meaningful frequency is actually much less. In a typical application such as our ECR simulations, Δz may be about 1 cm, and $v_e/\Delta z$ of the order of 10^8 sec^{-1}, as compared to ω_p of order 10^{11} sec^{-1}.

We next examine the mode structure when $c_s \neq 0$. To perform the integrals simply in closed form, we assume that $F_0(v)$ is a Lorentzian distribution,

$$F_0(v)=\frac{1}{\pi}\frac{v_e}{v^2+v_e^{\,2}}. \tag{20}$$

Then Eq. (18) becomes

$$1-\frac{k^2 c_s^{\,2}}{\omega^2}=-\frac{2}{\pi}\int_{-\infty}^{\infty}\frac{dx\,x(1-x^2)}{(1+x^2)^2(x-\Omega)}, \tag{21}$$

where $x \equiv v/v_e$ and $\Omega \equiv \omega/kv_e$. The contour for the integral in Eq. (21) can be closed above, and according to causality the pole at $x = \Omega$ is to be enclosed in the contour, even if $\mathrm{Im}\,\Omega$ is negative. Using the method of residues, Eq. (21) reduces to

$$1 - \frac{m_e}{m_i}\frac{1}{\Omega^2} = 2\frac{2\Omega^2 - i\Omega(1-\Omega^2)}{(1+\Omega^2)^2}. \tag{22}$$

If we multiply out the denominators in (22), we obtain a sixth order polynomial equation,

$$\Omega^2(1+\Omega^2)^2 - 4\Omega^4 + 2i\Omega^3(1-\Omega^2) = \frac{m_e}{m_i}(1+\Omega^2)^2. \tag{23}$$

We know that two of the roots lie at $\Omega = \pm 1$ if $m_e/m_i \to 0$. Assuming that these two roots lie close to ± 1, a perturbative solution gives

$$\omega = kv_e\left(\pm 1 + i\frac{m_e}{m_i}\right). \tag{24}$$

These modes are thus seen to be slightly unstable, by order m_e/m_i. This is not significant; the mode growth is so slow that it is obliterated by any of a number of incoherence effects (and in fact the entire formalism is based on neglect of higher order in m_e/m_i.) For example, we shall see in the next subsection that even the slightest degree of spatial smoothing damps the mode.

Next, we look for low frequency modes with $|\Omega| \ll 1$. Keeping only lowest order in Ω in the real and imaginary terms of Eq. (23), we find one pair of low-frequency roots,

$$\omega = kc_s\left(\pm 1 - i\sqrt{\frac{m_e}{m_i}}\right). \tag{25}$$

These are the ion sound modes, with the correct dispersion relation in the limit $\lambda_D \to 0$, and with the correct representation of electron Landau damping for the Lorentzian distribution (20). We show in the Appendix that when a complete Vlasov treatment is used, both electron and ion Landau damping terms appear correctly, and ion sound instability is also correctly represented if there is electron-ion streaming.

The last two roots of the sixth-order equation (23) are a double root at $\Omega = i$. However, this is a spurious root, which is not a root of the original equation (22). Thus the formalism supports only two pairs of modes. One pair is the ion sound mode, correctly represented. The second pair of modes are the (unphysical, but essentially stable) high frequency modes which tightly couple n_e to n_i and thus preserve quasineutrality.

B. Effect of Spatial Smoothing

In practice, we find that it is necessary to apply some spatial smoothing to the electric field,[27] to overcome the fluctuations introduced by particle statistics and enhanced by the derivative operation in Eq. (4). One might wonder about the effect of smoothing on the stability of the scheme. Thus we reexamine the mode structure in the presence of smoothing.

The smoothed electric field $\tilde{E}$ may be represented as

$$\tilde{E}(z) = \int_{-\infty}^{\infty} dz' \, K(z - z') \, E(z') , \tag{26}$$

where E(z) is given by

$$-eE(z) = \frac{\partial T_e}{\partial z} + \frac{T_0}{n_0} \frac{\partial n_i}{\partial z} , \tag{27}$$

and K(z-z′) is some symmetric kernel normalized to unity. In Fourier representation, the convolution becomes simply

$$-e\tilde{E}_k = -eE_k K_k = ikK_k T_e + ikK_k \frac{T_0}{n_0} n_i . \tag{28}$$

Note that the Fourier transform K_k is always real, and $1 \geq |K_k|$ for all k. If the width of the smoothing kernel K(z) is narrow compared to k^{-1}, then $K_k \rightarrow 1$ and the effect of smoothing vanishes. Using (28) in place of (11), we can retrace the derivation of the dispersion relation (22). We obtain the modified form

$$1 - K_k \frac{m_e}{m_i} \frac{1}{\Omega^2} = 2K_k \frac{2\Omega^2 - i\Omega(1-\Omega^2)}{(1+\Omega^2)^2} . \tag{29}$$

Equation (29) can be solved in the same way as (22). Again, there are four genuine roots. The two high-frequency modes which couple the electrons to the ions are now

$$\omega_k = kv_e \left[\pm \sqrt{(2-K_k)K_k} - i(1-K_k) + order\left(\frac{m_e}{m_i}\right) \right] . \tag{30}$$

These modes are now seen to be damped as long as $1-K_k > \text{order}\,(m_e/m_i)$, so the electrons should follow the ions in a quiescent fashion. The two low-frequency solutions of (29) are

$$\omega_k = kc_s K_k^{1/2} \left(\pm 1 - iK_k^{3/2} \sqrt{\frac{m_e}{m_i}} \right) . \tag{31}$$

Thus, as might be expected, the ion sound waves experience a reduction in frequency and in Landau damping, if there is smoothing on a scale comparable to the wavelength.

Obviously, if one wishes to resolve sound waves of a given wavelength, smoothing should only be applied on smaller spatial scales.

4. Numerical Implementation

The choice of time steps is limited by a number of considerations, in addition to the obvious requirement that the time step resolve any time scale of interest, such as a wave period. (i) Accuracy requires that during a single time step, particles not traverse a range over which the electric field, or other macroscopic variables, change significantly. (ii) If collisions are an important aspect of the problem, and Monte Carlo methods are used to model them, the time steps for each species must also be limited to a fraction of the collision time. Both of these conditions typically allow the ion time step to be longer than the electron time step by a factor of the order of $(m_i/m_e)^{1/2}$. (iii)In addition, we have seen that Eq. (4) couples the electrons to the ions by inducing rapid stable electron oscillations with phase velocity equal to the electron thermal velocity v_e. Since these oscillations can be excited by statistical fluctuations in a single cell, a conservative procedure to avoid numerical difficulties is to choose the electron time step no larger than the cell size divided by v_e, and to recalculate the electric field acting on the electrons at each electron time step. In practice, we have found that these conditions should be satisfied in the most stressing situations, such as the collisionless simulations presented later in this paper. Collisional situations generally are more forgiving, and appear often to allow longer time steps. Thus, to summarize, we use relatively long ion time steps, chosen to satisfy conditions (i) and (ii), and subdivide these time steps, typically by a factor of the order of $(m_i/m_e)^{1/2}$, to obtain electron time steps that satisfy all three conditions. These conditions permit electron time steps that are typically three orders of magnitude larger than the time steps $\Delta t < 2/\omega_p$ that are needed for conventional PIC codes. The ion time steps are even larger, and in addition the spatial grid scales can be orders of magnitude larger than λ_D.

The electric field is calculated as a grid quantity at each electron time step, from Eq. (4), or Eq. (10) if the plasma is magnetized. This electric field is then applied directly

to the electrons at each time step. To push the ions over a long ion time step, an electric field is used which is simply the average of the electric fields at each of the electron time steps during this ion time step. Thus there is significant temporal smoothing of Eq. (4) or (10), primarily a smoothing of the fluctuations in T_e, which helps to reduce statistical fluctuations in the ion motion.

The electrostatic potential energy of the plasma is $\int dV \left(n_i - n_e\right) e\phi$, and therefore is zero to the extent that exact quasineutrality is maintained. Thus, in the absence of inelastic scattering, the total kinetic energy should be conserved. This presumes, of course, that the electrons and ions see exactly the same electric field. However, energy conservation is preserved even if the electrons are pushed subject to the instantaneous electric field, and the ions to a time-averaged field, as long as the time averaging is properly centered over the ion time step. In practice, the oscillation of the electrons about the ion density profile means that quasineutrality is not exactly satisfied at any given time step, and correlations are possible which lead to long-term drifts in the total kinetic energy. However, these are very slow and can be controlled by giving proper attention to maintaining a sufficient number of simulation particles and adequate spatial smoothing. Some examples will be given.

For the collisionless examples below, we have used a large number of particles per grid point, ranging from an average of 500 particles per cell for free expansion to 2400 per cell for the ion acoustic wave. However, in our 2D ECR simulation code, where there is significant electron collisionality, we get good results with about 200 particles per cell. We use a linear laydown for both the electrons and the ions. The ion density and the pressure are smoothed using standard filtering techniques.[1] The algorithm for pushing the particles is a centered difference scheme. The electrons are subcycled with typically 32 electron time steps for each ion time step. For the examples shown here, the system is periodic, but in our ECR code the same method is used for a bounded system.

5. An Example: Free Expansion of a Plasma

To illustrate the use of the quasineutral formulation, we consider a test problem which can be solved exactly, and also can be solved analytically within our formulation. Consider the free expansion of a plasma consisting of hot isothermal electrons and cold ions, beginning with a Gaussian spatial profile in one dimension:

$$f_i(z,v,0) = \frac{1}{\sqrt{\pi}L_0}\exp\left(-\frac{z^2}{{L_0}^2}\right)\delta(v), \tag{32a}$$

$$f_e(z,v,0) = \frac{1}{\sqrt{\pi}L_0}\sqrt{\frac{m_e}{2\pi T_{0e}}}\exp\left(-\frac{z^2}{{L_0}^2}-\frac{m_e v^2}{2T_{0e}}\right). \tag{32b}$$

Even though this is a problem that is easily solved analytically, it poses a stiff challenge to a particle simulation, since there is a wide range in plasma density, and we assume there are no collisions. (Collisions make it much easier to implement this type of technique, by smoothing out statistical fluctuations.)

A. Analytic Treatment: Exact Quasineutrality

An exact solution to the Vlasov equation, with initial conditions specified by Eqs. (32), can be found in closed form. It corresponds to self-similar isothermal expansion,

$$f_i(z,v,t) = \frac{1}{\sqrt{\pi}L_i(t)}\exp\left(-\frac{z^2}{{L_i}^2(t)}\right)\delta\left(v-\frac{z\dot{L}_i(t)}{L_i(t)}\right), \tag{33a}$$

$$f_e(z,v,t) = \frac{1}{\sqrt{\pi}L_e(t)}\sqrt{\frac{m_e}{2\pi T_e(t)}}\exp\left[-\frac{z^2}{{L_e}^2(t)}-\frac{m}{2T_e(t)}\left(v-\frac{z\dot{L}_e(t)}{L_e(t)}\right)\right]. \tag{33b}$$

The expansion is driven by the electron pressure, with the ions dragged along by the electrostatic field. Thus a complete solution, using Poisson's equation, would show that $L_e(t)$ is larger than $L_i(t)$ by a small amount of the order of the Debye length. But to the extent that quasineutrality is observed, $L_e(t) = L_i(t)$, and $L_i(t)$ and $T_e(t)$ are determined by conservation of momentum and energy as the solutions to

$$\ddot{L}_i(t) = \frac{2T_e(t)}{m_i L_i(t)}, \tag{34a}$$

$$T_e(t) = T_e(0) - \frac{1}{2} m_i \dot{L}_i^{\,2}(t). \tag{34b}$$

Equations (34) can be solved for $L_i(t)$ in closed form. For the initial conditions specified by Eq. (32), the solution is

$$L_i(t) = \sqrt{L_0^{\,2} + 2c_{s0}^{\,2} t^2}\,. \tag{34c}$$

B. Analytic Treatment Using Our Model

Within our model, with E given by Eq. (4), it is easy to show that the electrons and ions each expand self-similarly, as in Eqs. (33), but with $L_e(t)$ not exactly equal to $L_i(t)$. $L_i(t)$ and $T_e(t)$ are given by Eqs. (34), but $L_e(t)$ is given by

$$\ddot{L}_e = 2v_e^{\,2}\left(\frac{1}{L_e} - \frac{L_e}{L_i^{\,2}}\right). \tag{35}$$

Rewriting Eq. (35) in terms of $\Delta \equiv (L_e - L_i)/L_i$, and subtracting (34a) from (35) gives

$$\ddot{\Delta} = -\frac{2v_e^{\,2}}{L_i^{\,2}}\left(\frac{(2+\Delta)\Delta}{1+\Delta} + \frac{m_e}{m_i}\right). \tag{36}$$

The first term of Eq. (36) causes Δ to oscillate about an equilibrium point. The second term causes a very small offset to the equilibrium point. (Interestingly, this offset is negative, so that in this formulation the ions lead the electrons by a displacement of order m_e/m_i.) Thus it is reasonable to assume $|\Delta| << 1$ and simplify (36) to

$$\ddot{\Delta} = -\left(\frac{2v_e(t)}{L_i(t)}\right)^2 \Delta . \tag{37}$$

Equation (37) indicates that Δ oscillates at the rapid frequency $\omega_0 = 2v_e/L_i(t)$, and since ω_0 is fast compared to the time scale for ion motion, these can be considered to be simple harmonic oscillations at a slowly varying frequency. These oscillations are not physical; they are the mechanism for coupling the electrons to the ions within our quasineutral formulation (4). However, they are stable oscillations which normally maintain a very small amplitude (in fact, comparable to the statistical fluctuations that would otherwise be present due to the finite number of particles), and thus are of no real significance. As mentioned earlier, a conservative condition for numerical stability is that the time step be less than ω_0^{-1}, and in fact, since statistical fluctuation can occur on length scales down to a single cell size Δz, less than $\Delta z/v_e$.

C. Numerical Simulation

Figures 1-3 show the results of a numerical simulation of the free expansion problem, for a hydrogen plasma (m_i/m_e = 1836). However, it was not possible in the simulation to allow the plasma to expand into a true vacuum, since the electric field from Eq. (4) depends on the reciprocal of the plasma density. (The noisy electric field in regions with very low density eventually dominates the problem.) In order to control the noise, we added a low density floor (5% of the peak density) to the Gaussian density profile as can be seen in Fig. 1a. We use 200,000 macroparticle electrons and an equal number of ions, in a 1D system 400 cells long.. The cell size is $\Delta z = 1$ cm. The system is initialized in accordance with Eq. (32), with $L_0 = 14$ cm and $T_e = 0.33$ eV. The time step

is $\Delta t = 25$ ns. Figure 1 shows the electron density profile (solid curve) and the ion density profile (dashed curve) at $t = 0$ and $t = 20$ μs. The deviations from quasi-neutrality are visible only at the peak density, and at the boundary with the low density background plasma. We note that the expansion is very nearly self-similar, as predicted. (Eventually, small deviations from self-similarity, due to the presence of the low-density background, become visible.) Figure 2 shows $L_i(t)$ from the simulation. The x's show the analytic solution (34c) for $L_i(t)$. We see that the expansion is smooth, and the analytic solution is well verified. Figure 3 shows plots of the total electron kinetic energy $W_e(t)$, the total ion kinetic energy $W_i(t)$, and the total kinetic energy $W(t)$. We note that the effect of the expansion is to convert the electron kinetic energy (which is nearly all thermal) to ion streaming energy. Overall kinetic energy is conserved to within 4%. To the extent that quasineutrality is maintained, there is essentially no potential energy, since the electron potential energy is always exactly the negative of the ion potential energy.

6. Second Example: Ion Sound

Ion sound with wavelength much greater than λ_D is a simple example of a plasma mode that occurs on the ion time scale and maintains quasineutrality. It is therefore not an easy mode to simulate with a standard PIC code using Poisson's equation and a realistic value of m_e/m_i. In Sec. 3 above, we used a simplified model (Vlasov electrons with Lorentzian distribution, cold fluid ions) to show that the ion sound mode is contained within our quasineutral model, and in the Appendix we provide a full Vlasov analysis that shows that the model gives exactly the correct dispersion relation, including electron and ion Landau damping terms. Here we show the results of simulations of ion sound within the nearly-linear and nonlinear regimes, with the mass ratio $m_i/m_e = 1836$.

A. Standing-Wave Ion Sound in the Linear Regime

We initiate an ion sound standing wave by loading initial particle densities

$$n_e = n_i = n_0 [1 + \alpha \sin(2\pi z/L)], \tag{38}$$

with the fluid velocities u_e and u_i initially zero for both species. The simulation is done with periodic boundary conditions in a 1D system of length $2L = 25$ cm, with cell length $\Delta z = 0.125$ cm; thus, there are two wavelengths within the box, and 100 cells per wavelength. The wave amplitude is taken to be $\alpha = 0.05$, and 2400 particles of each species are used, per cell. A very large number of particles is needed for this simulation to resolve the very small wave amplitude. The electron temperature is set to 1.33 eV, so that $v_e = 4.8\times10^7$ cm/sec, $c_s = 1.1\times 10^6$ cm/sec, and the wave period should be $L/c_s = 11.3$ μs. The ions are initially cold. The ion time step is 15.6 ns, and the electrons are subcycled 4 times per ion time step.

The temporal evolution of the fundamental (wavelength L) Fourier mode of n_e and n_i is shown in Fig. 4. The densities are taken from the Fourier transforms of the instantaneous values of $n_e(z)$ and $n_i(z)$ at the ion time step. We see that the wave period is 11.1 μs, in excellent agreement with the theoretical value. We note that at any given time, quasineutrality ($n_e = n_i$) holds to better than 5%. Plots of the spatial dependence of the wave (not shown) indicate that the two wavelengths contained within the box are exactly the same.

Equation (A9) predicts Landau damping at the rate 9% per wave period. However, in a one-dimensional ion sound wave, even at wave amplitude $\alpha = 0.05$, trapping of the resonant electrons interferes with Landau damping at a very early stage. The trapping frequency is $\omega_T = \sqrt{keE/m_e}$, and according to the linearized version of Eq. (4), $E = k\alpha T_e$. Thus

$$\omega_T = kc_s\sqrt{\alpha\frac{m_i}{m_e}} = 9.6\,kc_s, \tag{39}$$

and Landau damping should be over in a fraction of a wave period. The slight damping seen in Fig. 4 thus would seem to be the initial Landau damping, followed by a slower damping due to mode coupling to higher harmonics. The second harmonic (wavelength L/2) grows to a level of 10% of the fundamental after two periods, as shown in Fig. 4. This is in reasonable agreement with simple two-mode coupling theory, which predicts 15% at this time, and consequent damping of the fundamental by about 1.5%. From a computational point of view, it is worth noting that the rate of mode coupling is found to be quite sensitive to the grid spacing. The simulation of Fig. 4, with 100 grid points per wavelength, shows qualitative agreement with theory, but a calculation with 25 grid points per wavelength shows substantially faster second harmonic growth and decay of the fundamental.

B. Nonlinear Traveling Wave

The nonlinear evolution of a standing wave is complex, but for traveling sound waves an analytic solution is possible via the method of characteristics.[28] Since λ_D is set to zero within our model, the ion sound waves are nondispersive, and therefore the mode coupling theory is essentially the same as that of ordinary sound waves in a neutral gas,[28] with T_e playing the role of the gas temperature. (However, ion sound waves are isothermal,[29] whereas sound waves in a molecular gas are adiabatic. Therefore the adiabatic constant γ must be set to unity in the ion sound theory.) The velocity is found to be the solution of the implicit equation

$$u(z,t) = u\big(z - u(z,t)\big). \tag{40}$$

It is well known that Eq. (40) leads to steepening of the density and velocity profiles, and ultimately to wave breaking when $\partial u/\partial z$ becomes infinite. For an initial sinusoidal profile

$$\frac{u(z,0)}{c_s} = \alpha \sin\left(\frac{2\pi z}{L}\right), \tag{41}$$

this occurs when

$$t = t_{break} = \frac{L}{2\pi\alpha c_s}. \tag{42}$$

In Fig. 5 we show the results of a simulation similar to those of the previous subsection, except that the wave amplitude is larger at $\alpha = 0.20$ and a traveling wave is initiated by setting the initial ion fluid velocity as in Eq. (41). We note the steepening of the wave up to the point of breaking at about t = 9 μsec, in good agreement with the theoretical prediction t = 9.04 μsec. As the wave nears the breaking point, non-physical structure such as the ripple and sharp peak in Fig. 5b begin to appear. These features appear to be associated with finite spatial resolution, and limit the accuracy of determination of the breaking point by perhaps 1 μsec. After wave breaking, the quasineutral theory is no longer correct, since λ_D length scales are relevant to the subsequent evolution of the ion acoustic shocks.

7. Conclusions

We have presented a method for doing plasma simulations with particle electrons and particle ions, in the quasineutral limit. The method permits (indeed, it requires) the use of grid spacing long compared to λ_D and time stepping long compared to ω_{pe}^{-1}. We have demonstrated analytically that the method is stable (at least on a continuous time basis), and that it gives the correct dispersion relation for ion sound, including Landau resonance terms. We have also demonstrated the use of the method to simulate free expansion of a plasma, and linear and nonlinear ion sound.

We believe that the technique presented here should be useful for a variety of problems involving quasineutral plasmas. We are using this method in a 2D simulation code for magnetized plasmas, which includes in addition cross-field transport, sheaths at insulating or conducting walls, ECR heating, and collisions and chemistry. The techniques used to model these other aspects of the physics will be discussed in subsequent publications. The code runs for very long times (hundreds of μsec), with time steps typically on the order of 10 nsec, and with running time typically on the order of a few hours on a IBM RS6000 workstation.

Appendix: Vlasov Theory of Ion Sound

In this section we show analytically that our quasineutral formulation, using the approximate form (4) for **E**, gives exactly the correct dispersion relation for linearized ion sound waves, including even the Landau damping terms.

Review: Vlasov-Poisson Theory of Ion Sound

To clarify the issues involved, we begin with a brief review of the standard derivation of the ion sound dispersion relation from the linearized 1D Vlasov equation,

$$\frac{\partial f_\alpha}{\partial t} + v\frac{\partial f_\alpha}{\partial z} \mp \frac{n_0 eE}{m_\alpha}\frac{\partial F_{0\alpha}}{\partial v} = 0, \tag{A1}$$

with the upper sign for electrons and the lower sign for ions, and with the electric field E determined by Poisson's equation. Using a linearized normal mode representation for the perturbed part of the distribution function f_α, we find

$$f_{\alpha k}(v) = \pm\frac{in_0 eE}{m_\alpha}\frac{dF_{0\alpha}}{dv}\frac{1}{\omega - kv}, \tag{A2}$$

and the species densities $n_{\alpha k}$ are

$$n_{\alpha k} = \pm\frac{in_0 eE}{m_\alpha}\int\frac{dvF_{0\alpha}'(v)}{\omega - kv}. \tag{A3}$$

Inserting (A3) into Poisson's equation,

$$ikE_k = 4\pi(n_{ek} - n_{ik}), \tag{A4}$$

we obtain the dispersion relation,

$$0 = 1 - \frac{\omega_{pe}^2}{k^2}\int dv \frac{F_{0e}'(v)}{v - \omega/k} - \frac{\omega_{pi}^2}{k^2}\int dv \frac{F_{0i}'(v)}{v - \omega/k}\ , \qquad \text{(A5)}$$

where causality indicates that the contours in Eqs. (A3) and (A5) go below the pole at $v = \omega/k$. The usual dispersion relation for ion sound can be obtained by making several approximations in Eq. (A5). First assume that the imaginary part of ω/k is small. Let u (which may be zero) be the relative electron-ion drift, and assume that $F_{0i}(v)$ is a symmetric function of v, but F_{0e} is a symmetric function of $w \equiv v - u$. Assume that $T_e >> T_i$, $u << v_e$, and $v_i << \omega/k << v_e$. Then the first integral in Eq. (A5) can be treated by first extracting the contribution from the pole at $v = \omega/k$, and then expanding the remaining non-singular integral under the assumption that $\omega/k << |w|$ and $u << |w|$ for nearly all electrons:

$$\int \frac{dvF_{0e}'(v)}{v - \omega/k} \cong -i\pi F_{0e}'\left(v = \frac{\omega}{k}\right) + \int \frac{dwF_{0e}'(w)}{w}\left[1 + \frac{\omega/k - u}{w} + \left(\frac{\omega/k - u}{w}\right)^2\right]. \qquad \text{(A6)}$$

The second integral in Eq. (5) can be treated by first extracting the contribution from the pole, and then expanding the remaining integral under the assumption that $\omega/k >> |v|$ for nearly all ions:

$$\int \frac{dvF_{0i}'(v)}{v - \omega/k} \cong -i\pi F_{0i}'\left(\frac{\omega}{k}\right) - \frac{k}{\omega}\int dvF_{0i}'(v)\left(1 + \frac{kv}{\omega}\right) = -i\pi F_{0i}'\left(\frac{\omega}{k}\right) + \frac{k^2}{\omega^2}\ . \qquad \text{(A7)}$$

Keeping only the leading term in the expansion (A6) gives the dispersion relation,

$$0 = 1 - \frac{\omega_{pe}^2}{k^2}\int \frac{dwF_{0e}'}{w} - \frac{\omega_{pi}^2}{\omega^2} + \frac{k^2\omega_{pi}^2}{\omega^4}\int dvv^3F_{0i}' - \frac{i\pi}{k^2}\left[\omega_{pe}^2F_{0e}'\left(\frac{\omega}{k}\right) + \omega_{pi}^2F_{0i}'\left(\frac{\omega}{k}\right)\right]. \tag{A8}$$

In the case of Maxwellian velocity distributions, this reduces to the familiar form

$$\omega = \frac{kc_s}{(1+k^2\lambda_D^2)^{1/2}} + \frac{i\pi}{2}\frac{kc_s}{(1+k^2\lambda_D^2)^{3/2}}\left[\frac{T_e}{m_e}F_{0e}'\left(\frac{\omega}{k}\right) + \frac{T_e}{m_i}F_{0i}'\left(\frac{\omega}{k}\right)\right]. \tag{A9}$$

Quasineutral Derivation

In the quasineutral context, the electric field is determined by the linearized form of Eq. (4),

$$-eE_k = \frac{ikP_{ek}}{n_0} + \frac{ikP_{0e}}{n_0^2}\left(n_{ik} - n_{ek}\right), \tag{A10}$$

with

$$P_{ek} = \int dvf_{ek}(v)m_ev^2 = in_0eE\int \frac{dvF_{0i}'(v)}{\omega - kv}. \tag{A11}$$

Using Eqs. (A3) and (A11) in (A10), we obtain the dispersion relation

$$0 = 1 + \int \frac{dv\left(v^2 - v_e^2\right)F_{0e}'}{v - \omega/k} - c_s^2\int \frac{dvF_{0i}'}{v - \omega/k}. \tag{A12}$$

Equation (A12) looks different from Eq. (A8). Nevertheless, using the expansions (A6) and (A7) but keeping *all terms* shown in (A6) gives

$$0 = -\frac{\omega_{pe}^2}{k^2}\int \frac{dwF_{0e}'}{w} - \frac{\omega_{pi}^2}{\omega^2} + \frac{k^2\omega_{pi}^2}{\omega^4}\int dvv^3F_{0i}' - \frac{i\pi}{k^2}\left[\omega_{pe}^2F_{0e}'\left(\frac{\omega}{k}\right) + \omega_{pi}^2F_{0i}'\left(\frac{\omega}{k}\right)\right], \tag{A13}$$

Equation (A13) is identical to Eq. (A8), except for the absence of the first term on the RHS of (A8). This term is smaller than the other terms in (A8) by order $k^2\lambda_D^2$, and thus disappears in the quasineutral limit $k\lambda_D \to 0$.

References

1. C. K. Birdsall and A. B. Langdon, *Plasma Physics Via Computer Simulation* (Adam Hilger, Bristol, Philadelphia and New York, 1991).
2. R. W. Hockney and J. W. Eastwood, *Computer Simulation Using Particles* (Adam Hilger, Bristol and New York, 1988).
3. T. Tajima, *Computational Plasma Physics* (Addison-Wesley, Reading, MA, 1989).
4. See Ref. 1, p 56.
5. J. Denavit, J. Comput. Phys. **42**, 337 (1981).
6. R. J. Mason, J. Comput. Phys. **41**, 233 (1981).
7. A. Friedman, A. B. Langdon, and B. I. Cohen, Comments Plasma Phys. and Controlled Fusion **6**, 25 (1981).
8. A. B. Langdon, B. I. Cohen, and A. Friedman, J. Comput. Phys. **51**, 107 (1983).
9. J. U. Brackbill and B. I. Cohen, eds., *Multiple Time Scales* (Academic Press, 1985, Chapters 8, 9, 11).
10. D. W. Hewett and D. J. Lawson, J. Comput. Phys. **101**, 11 (1992).
11. See Ref. 1, pp. 339-345.
12. F. F. Chen, *Introduction to Plasma Physics* (Plenum Press, New York, 1974), p. 66.
13. J. K Lee and C. K. Birdsall, Phys. Fluids **22**, 1306, 1979.
14. R. J. Mason, in Ref. 16, Chapter 8.
15. H. Okuda, J. M. Dawson, A. T. Lin, and C. C. Lin, Phys. Fluids **21**, 476 (1978).
16. C. K. Birdsall, IEEE Trans. Plasma Sci. **19**, 65 (1991).
17. R. W. Boswell and I. J. Morey, Appl. Phys. Lett. **52**, 21 (1988).
18. D. Vender and R. W. Boswell, IEEE Trans. Plasma Sci. **18**, 725 (1990).
19. M. Surendra, D. B. Graves, and I. J. Morey, Appl. Phys. Lett. **56**, 1022 (1990).
20. R. K. Porteus and D. B. Graves, IEEE Trans. Plasma Sci. **19**, 204 (1991).
21. D. B. Graves, H. Wu, and R. K. Porteus, Japan, J. Appl. Phys. **32**, 2999 (1993).
22. V. P. Gopinath and T. A. Grotjohn, IEEE Trans. Plasma Sci. **23**, 602 (1995).
23. V. Vahedi, C. K. Birdsall, M. A. Lieberman, G. DiPeso, and T. D. Rognlien, Plasma Sources Sci. Tech. **2**, 261 (1993).
24. M. M. Turner and M. B. Hopkins, Phys. Rev. Lett. **69**, 3511 (1992).
25. K. A. Ashtiani, J. L. Shohet, W. N. G. Hitchon, G.-H. Kim, and N. Hershkowitz, J. Appl. Phys. **78**, 2270 (1995).
26. M. Lampe, G. Joyce, and W. M. Manheimer, *in Lectures in Plasma Physics and Technology* (ed. V. Stefan, La Jolla International School of Physics, 1996, in press).
27. See Ref. 1, p. 437.
28. Landau and Lifschitz, *Fluid Mechanics* (Addison-Wesley, Reading, MA. 1959), p. 366-386.
29. D. Montgomery, Phys. Rev. Lett. **19**, 1465 (1967).

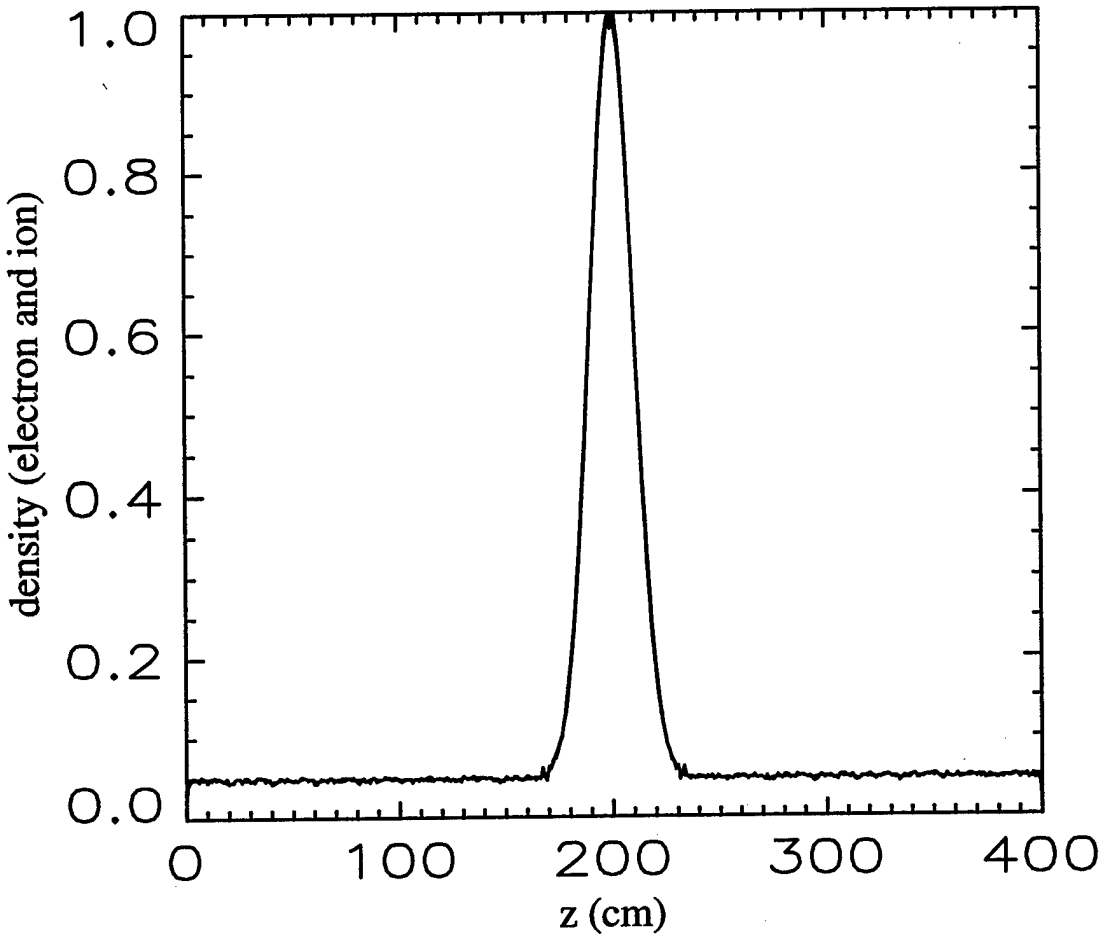

(a)

Fig. 1 — (a) Initial conditions for the free expansion simulation: $n_e(z)$ and $n_i(z)$ at t = 0. (b) $n_e(z)$ and $n_i(z)$ at t = 20 μsec. In both cases, $n_e(z)$ and $n_i(z)$ are essentially indistinguishable.

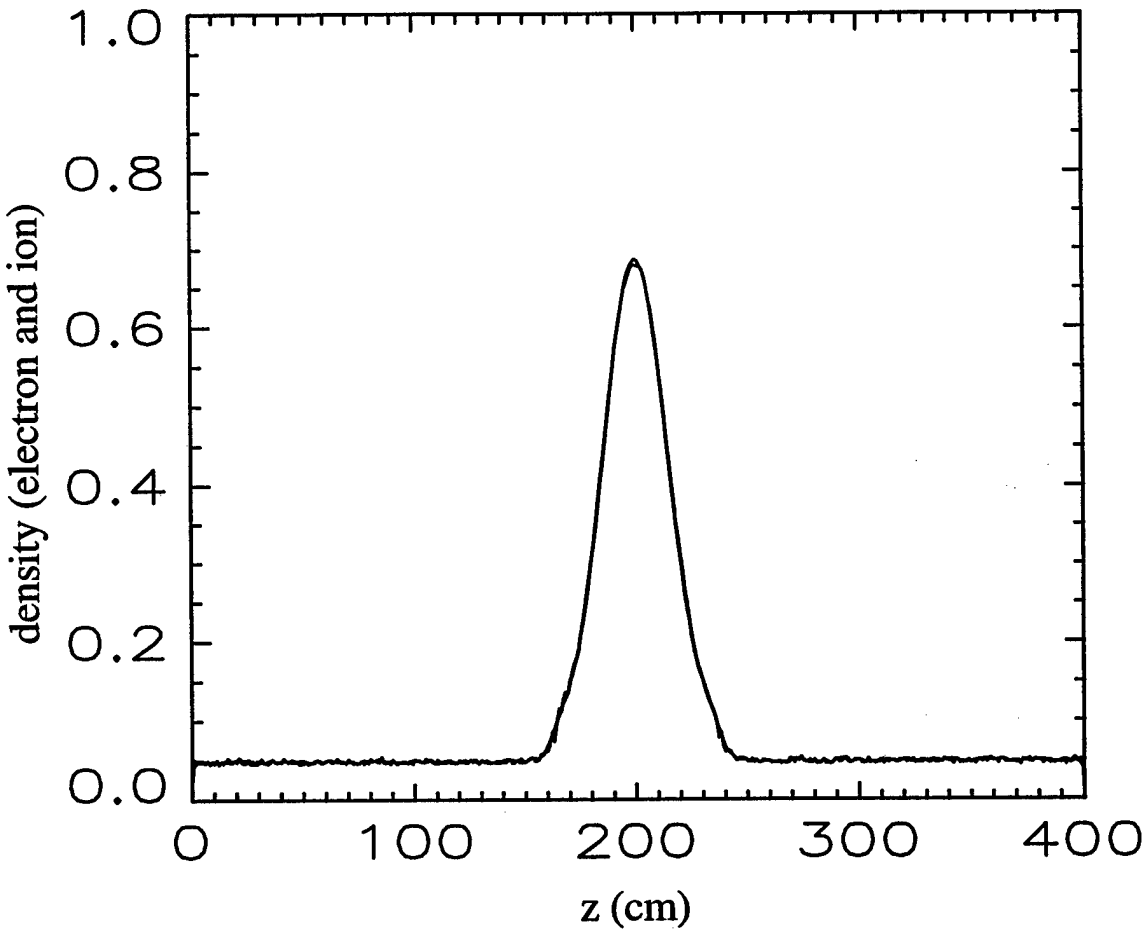

(b)

Fig. 1 (Continued) — (a) Initial conditions for the free expansion simulation: $n_e(z)$ and $n_i(z)$ at $t = 0$. (b) $n_e(z)$ and $n_i(z)$ at $t = 20$ μsec. In both cases, $n_e(z)$ and $n_i(z)$ are essentially indistinguishable.

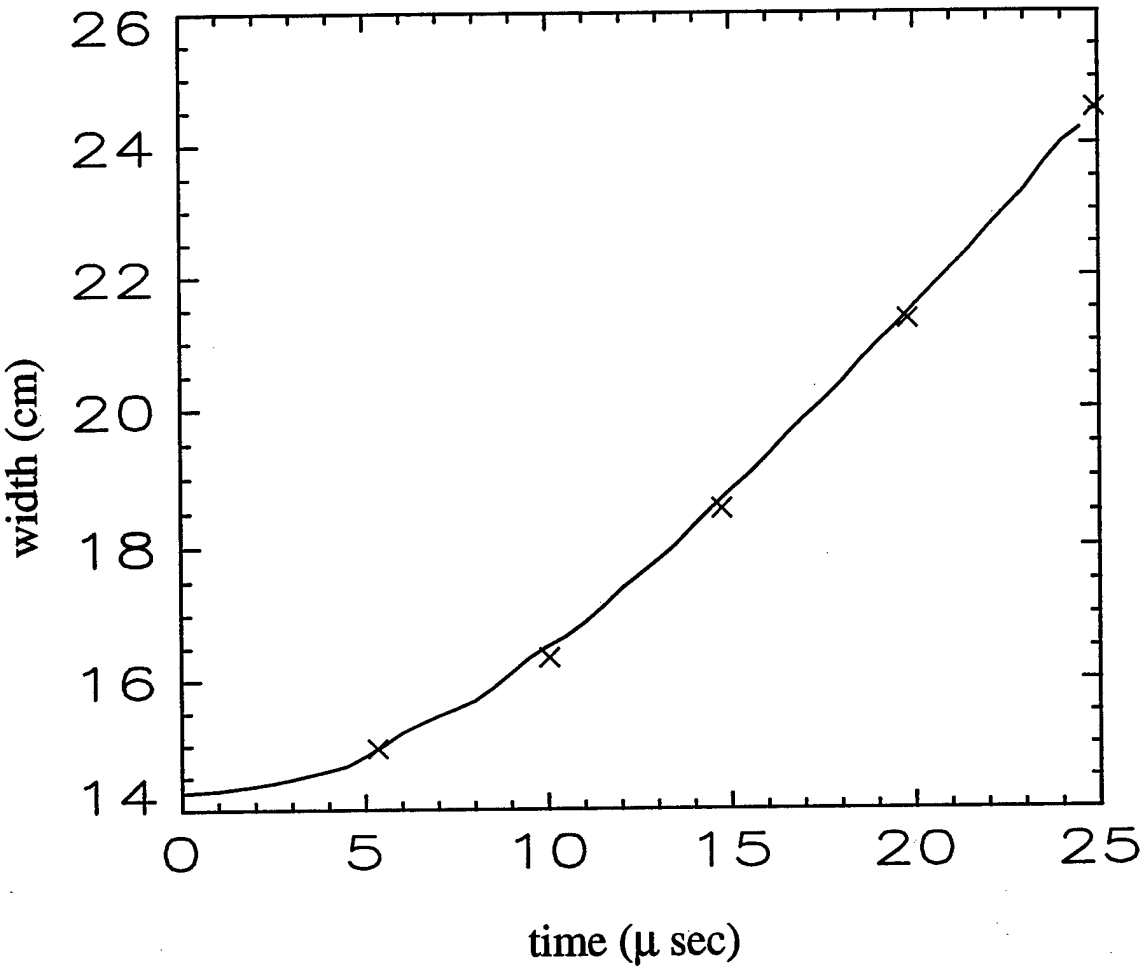

Fig. 2 — Simulation result for expansion of the ion characteristic with $L_i(t)$. The x's are the analytic result (34c).

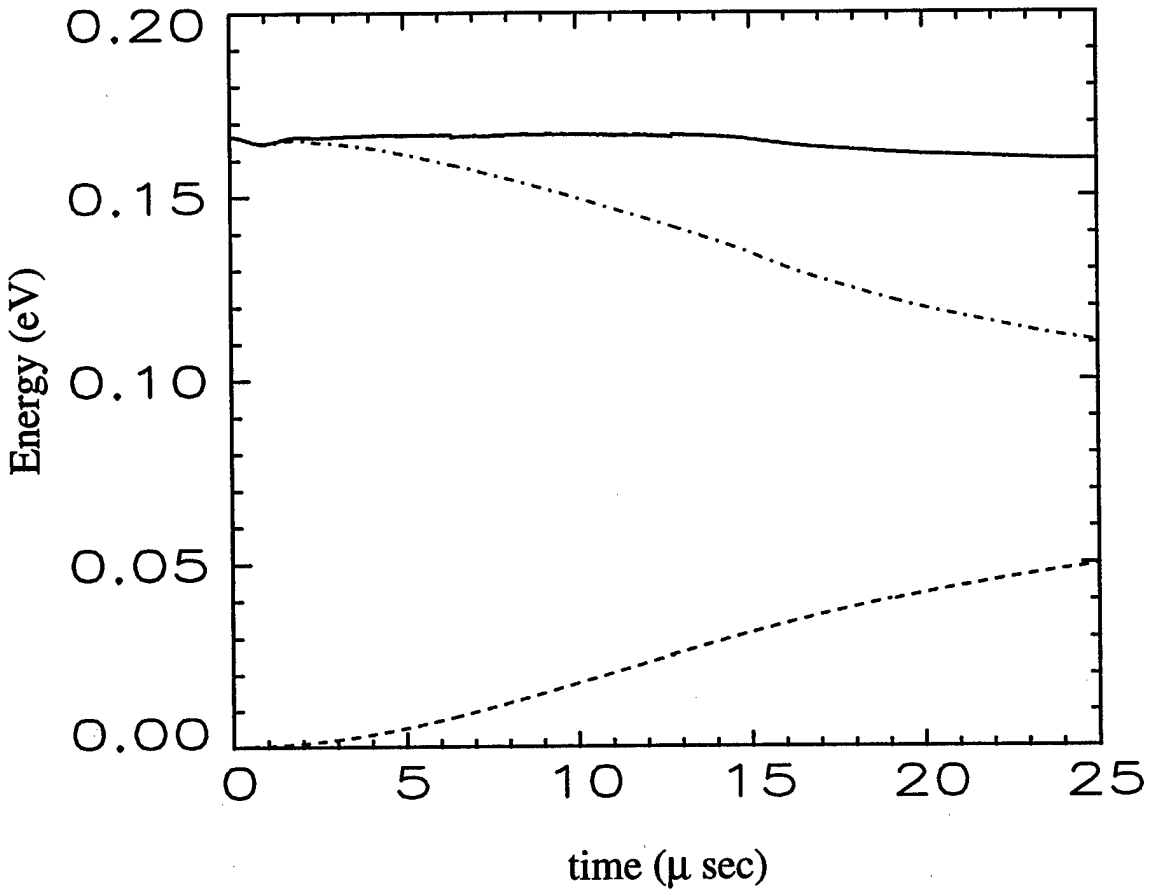

Fig. 3 — Time dependence of the electron kinetic energy $W_e(t)$ (dot-dashed curve), ion kinetic energy $W_i(t)$ (dashed curve), and total kinetic energy W(t) (solid curve) during free expansion.

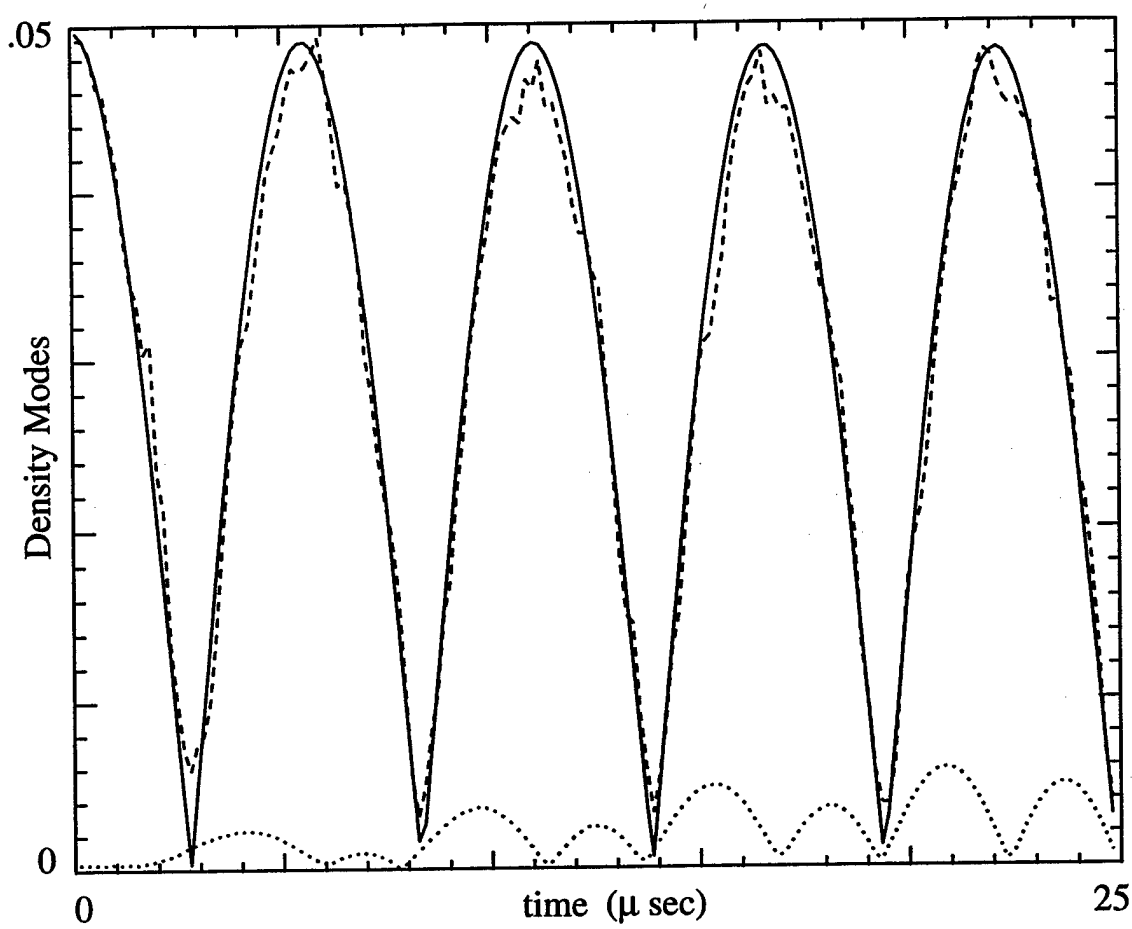

Fig. 4 — Temporal evolution of the standing ion sound wave: electron density fundamental mode (solid curve), ion density fundamental mode (dashed curve), and electron density second harmonic mode (dotted curve). Each of the curves plots the absolute value of the wave amplitude.

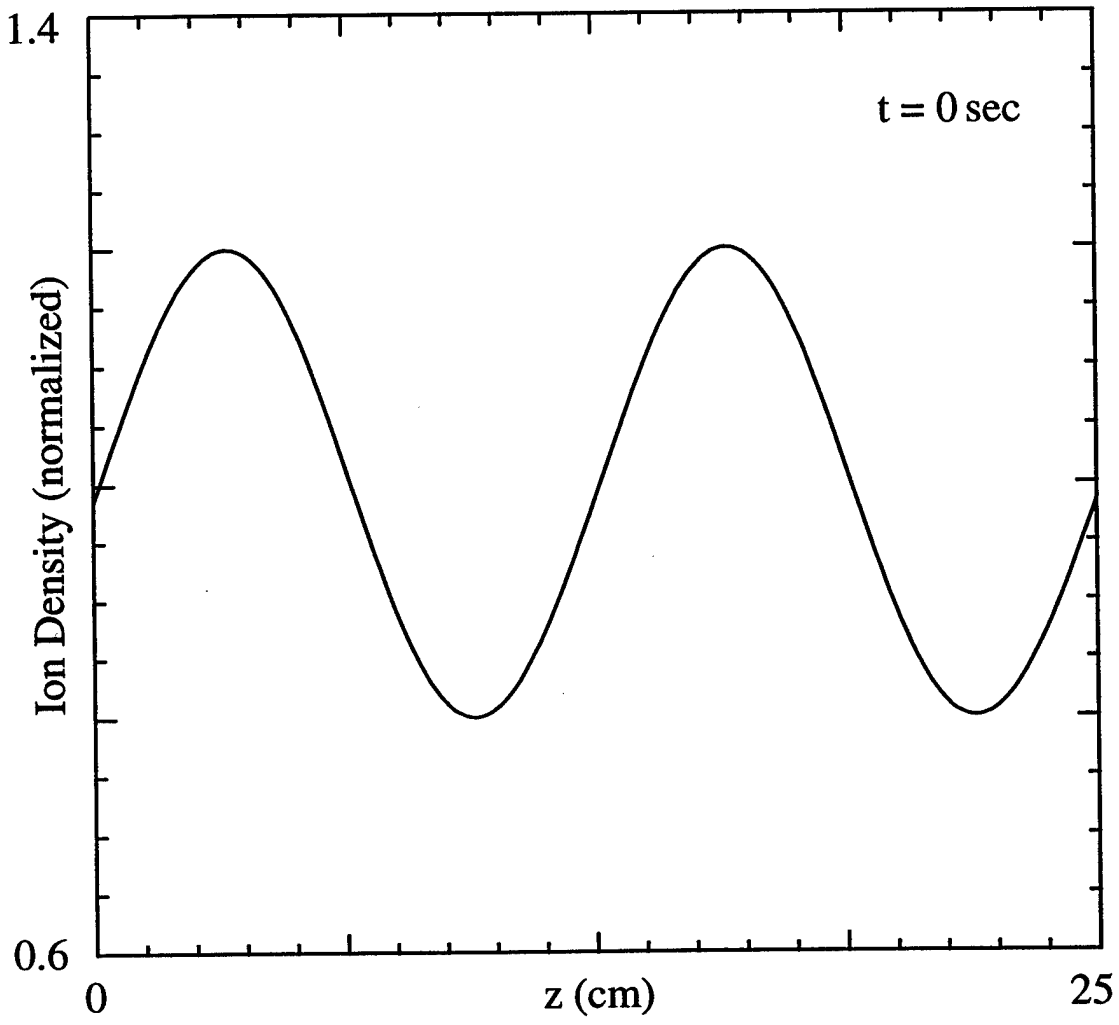

(a)

Fig. 5 — Density profiles showing steepening of the traveling ion sound wave: (a) t = 0, (b) t = 5.75 μsec, (c) t = 9.0 μsec.

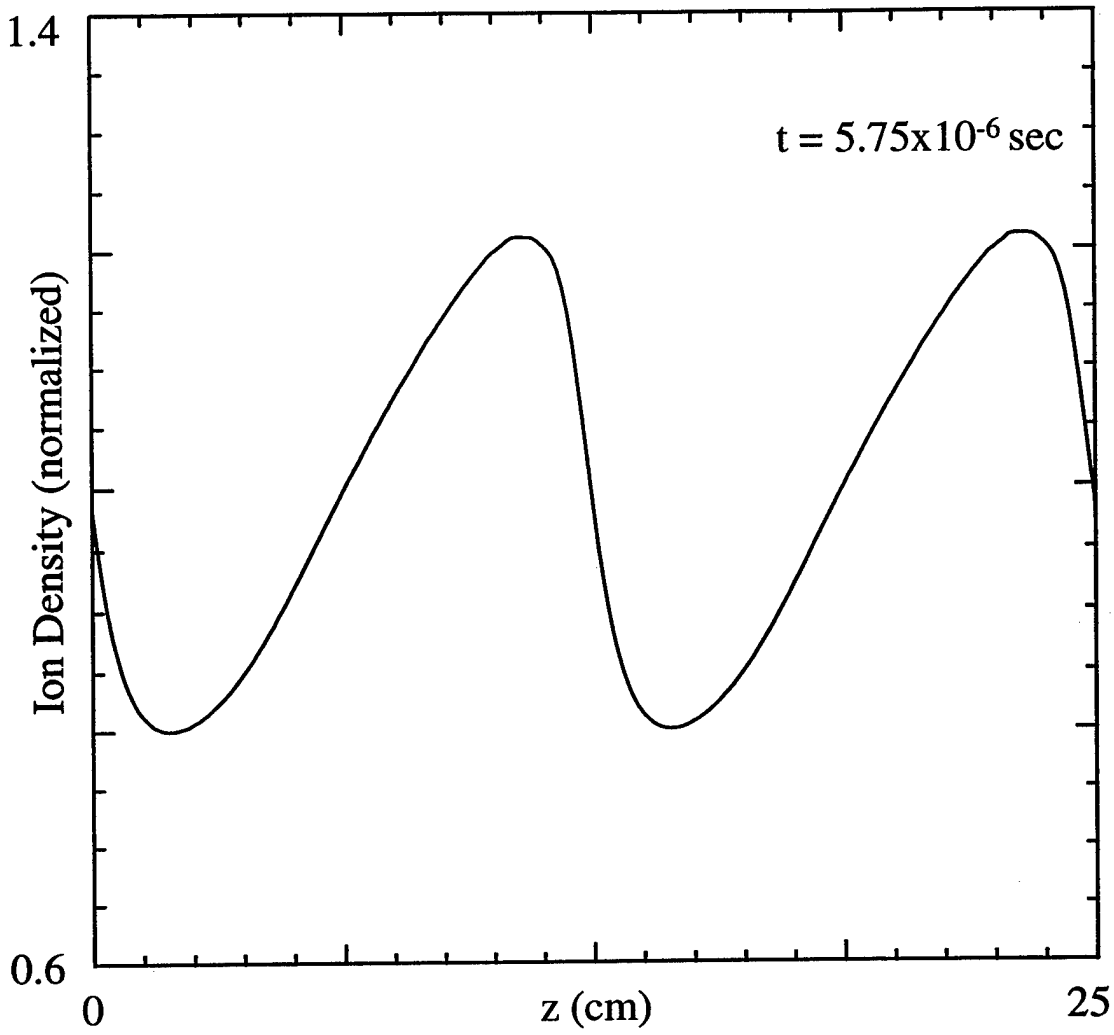

(b)

Fig. 5 (Continued) — Density profiles showing steepening of the traveling ion sound wave: (a) t = 0, (b) t = 5.75 μsec, (c) t = 9.0 μsec.

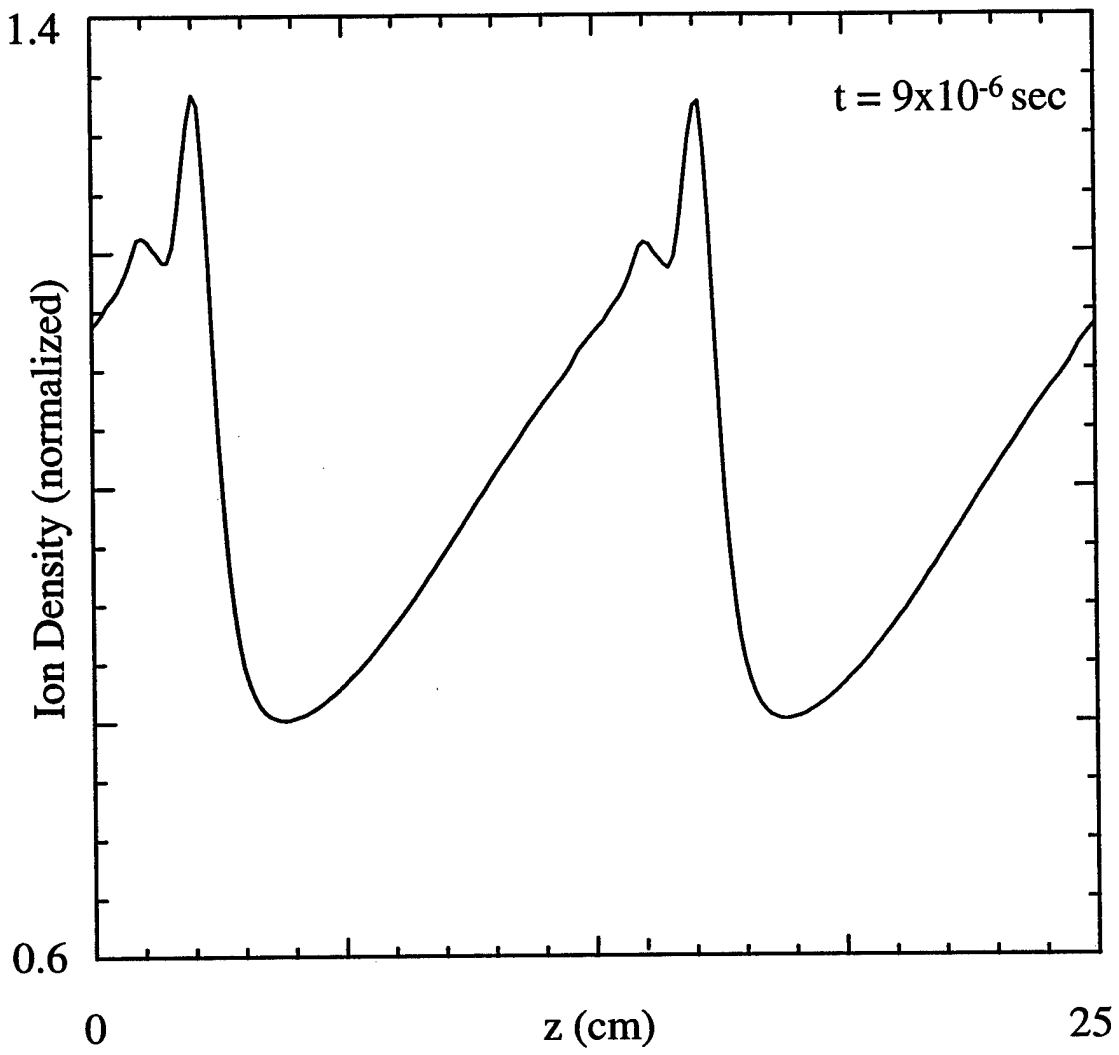

(c)

Fig. 5 (Continued) — Density profiles showing steepening of the traveling ion sound wave: (a) t = 0, (b) t = 5.75 μsec, (c) t = 9.0 μsec.